5-2022

Structures and Regulations of Translation Initiation Factors in *Pseudomonas aeruginosa* Protein Biosynthesis to Develop New Potential Antimicrobial Agents

Nicolette Valdez
The University of Texas Rio Grande Valley

STRUCTURES AND REGULATIONS OF TRANSLATION INITIATION FACTORS IN *PSEUDOMONAS AERUGINOSA* PROTEIN BIOSYNTHESIS TO DEVELOP NEW POTENTIAL ANTIMICROBIAL AGENTS

A Thesis

by

NICOLETTE VALDEZ

Submitted in Partial Fulfillment of the

Requirements for the Degree of

MASTER OF SCIENCE

Major Subject: Biochemistry and Molecular Biology

The University of Texas Rio Grande Valley

May 2022

STRUCTURES AND REGULATIONS OF TRANSLATION INITIATION FACTORS IN *PSEUDOMONAS AERUGINOSA* PROTEIN BIOSYNTHESIS TO DEVELOP NEW POTENTIAL ANTIMICROBIAL AGENTS

A Thesis
by

NICOLETTE VALDEZ

COMMITTEE MEMBERS

Dr. Yonghong Zhang
Chair of Committee

Dr. Xiaoqian Fang
Committee Member

Dr. Arnulfo Mar
Committee Member

Dr. Shizue Mito
Committee Member

May 2022

ABSTRACT

Valdez, Nicolette, Structures and Regulations of Translation Initiation Factors in Pseudomonas aeruginosa Protein Biosynthesis to Develop New Potential Antimicrobial Agents. Master of Science (MS), May, 2022, 42 pp., 1 table, 12 figures, references, 64 titles.

The treatment and eradication of infectious diseases caused by multidrug resistant pathogens has become increasingly difficult and results in inadequate therapy for those affected. *Pseudomonas aeruginosa* is an opportunistic pathogen, primarily known for infecting immunocompromised individuals and being the leading cause of morbidity and mortality in cystic fibrosis patients. Highly evolved antibiotic resistance mechanisms in *P. aeruginosa* make it difficult to eliminate infections of this pathogen without producing further damage to the hosts. This results in an unmet need for the development of new antimicrobial agents.

Translation initiation factors present in the protein biosynthesis pathway of *P. aeruginosa* were investigated. A synthetic peptide was designed and utilized as a functional mimic of IF1 in *P. aeruginosa* and displayed antimicrobial activity. Additionally, the N-terminal domain of IF3 in *P. aeruginosa* was investigated for insight into the role of this protein in protein synthesis so that it may provide a clue for the rational design of new antimicrobials.

DEDICATION

The completion of my master's degree would not have been possible without the love and support of my family. To my mother, Blanca Valdez, my father, Juan Valdez, and my siblings, Kathy and JC, thank you for your love, patience, and continued motivation.

ACKNOWLEDGMENTS

Foremost, I would like to express my sincere gratitude to my advisor, Dr. Yonghong Zhang, for his continuous support and patience throughout the completion of my thesis. He continuously challenged me academically and pushed me to be a better student and researcher with his immense knowledge. The professional and personal growth that has come out of this research experience is something I will value as I continue to pursue my career goals.

I would also like to thank my thesis committee, Dr. Xiaoqian Fang, Dr. Arnulfo Mar, and Dr. Shizue Mito, for their guidance, patience, and cooperation throughout the completion of my thesis. Additionally, we would like to thank Dr. Frank Dean for providing the Trevigen TACS MTT Cell Proliferation Assay Kit.

Lastly, I would like to thank my lab members for their assistance and friendship that helped make this experience more memorable.

TABLE OF CONTENTS

Page

LIST OF FIGURES

Page

CHAPTER 1

INTRODUCTION

1.1 Statement of The Problem

The abuse and misuse of antibiotics has heightened the development of multi-drug resistant (MDR) pathogens (Girard and Bloemberg, 2008; Wang et al., 2019). MDR pathogens are now recognized as one of the primary sources of nosocomial, or hospital-acquired infections (HAI). One of the most frequently isolated MDR pathogens in hospitalized individuals is *Pseudomonas aeruginosa*. *P. aeruginosa* is a Gram-negative, opportunistic pathogen responsible for chronic lung infections in cystic fibrosis (CF) patients. The accumulation of mucus or sputum in the lungs of CF patients creates a favorable environment for *P. aeruginosa* pathogenicity resulting in reduced pulmonary function and the leading cause of morbidity and mortality in these individuals (Palmet et al., 2021; Rossi et al., 2021). Nearly 47% of adult CF patients in the United States (US) experience a *P. aeruginosa* infection (Reece et al., 2017). *P. aeruginosa* is one of the major pathogens involved with HAI, especially in cancer, burn, and intensive care units (Burrows, 2018). Moreover, it is responsible for many eye infections relating to the formation of biofilms on contact lenses and ear infections (Cope et al., 2016). Infections linked to *P. aeruginosa* are often accompanied by chronic inflammation, deterioration of lung function, and an overall worsened quality of life (Li et al., 2020). *P. aeruginosa* is frequently associated with respiratory infections, urinary tract infections, and is responsible for 10.6% of pneumonia

cases since 2016, including hospital-acquired and ventilator-associated pneumonia (Suetens et al., 2018; Guillamet et al., 2016). As of 2019, deaths associated with this pathogen have increased by 80% since 2013 with an estimated $767 million in attributable healthcare costs, thus the Center for Disease Control (CDC) has characterized *P. aeruginosa* as a serious public health threat requiring prompt and sustained action (CDC, 2019).

1.2 Statement of The Purpose

Bacterial protein synthesis is an essential metabolic process and has been a validated target for antimicrobial development as seen in the development of the macrolide and aminoglycoside family of antibiotics (Valdez et al., 2021; McCoy et al., 2011). Translation initiation in prokaryotes is the most regulated and the rate-limiting step in protein synthesis (Arenz and Wilson, 2016). Three initiation factors facilitate translation initiation and act to promote the formation of the 30S initiation complex, a critical step that marks the beginning of protein synthesis. Few therapeutic options against *P. aeruginosa* infections have been successful because of its prompt ability to develop resistance to most antibiotics. Although new therapeutic strategies have been implemented to help combat infections of MDR pathogenic bacteria there is still an unmet need for the discovery of new compounds distinctive from present antimicrobials. The focus of this research was to investigate the structures and regulations of translation initiation factors IF1 and IF3 of *P. aeruginosa*. Understanding the functional and structural aspects of IF1 and IF3 will provide a more in depth understanding of protein synthesis in *P. aeruginosa*. Through an innovative combination of biophysical techniques, development of broad-spectrum antimicrobial peptides with the potential to inhibit bacterial growth will have profound implications for alternative antimicrobial therapies against this pathogen.

CHAPTER II

REVIEW OF LITERATURE

2.1 Development of Pathogenesis in *Pseudomonas Aeruginosa*

The versatile pathogenicity of *P. aeruginosa* can be attributed to the highly evolved resistance mechanisms continuously developed within the pathogen and the large and variable antibiotic resistance determinants present within its genome (Jurado-Martin et al., 2021). *P. aeruginosa* contains an extensive number of virulence factors at its disposal and various strains of this pathogen utilize their high levels of intrinsic, acquired, or adaptive resistance mechanisms to counter most antibiotics (Pang et al., 2019; Jurado-Martin et al., 2021). In addition, high-risk clones of *P. aeruginosa* contain multiple chromosomal determinants and complex regulatory pathways that can provide resistance to antibiotics to which it has never been exposed (Winkler et al., 2015).

P. aeruginosa possesses a high level of intrinsic resistance naturally available within its genome. Antibiotics such as the β-lactam family of antibiotics (penicillin, carbapenem, cephalosporin, etc.) bind to the penicillin-binding proteins involved in peptidoglycan synthesis and thereby block bacterial cell wall biosynthesis (Pandey and Cascella, 2021). Moreover, aminoglycoside antibiotics (gentamicin, tobramycin, and amikacin) inhibit bacterial protein synthesis by binding to the A-site on the 30S ribosome or inhibiting messenger RNA (Krause et al., 2016). The quinolone family of antibiotics (levofloxacin and ciprofloxacin) inhibit DNA

gyrase and Topoisomerase IV to block bacterial DNA replication (Aldred et al., 2014). In addition to the aforementioned antibiotics, the mechanism of action of other widely used antibiotic families requires the penetration of the cellular membrane. An intrinsic resistance mechanism within *P. aeruginosa* is an impermeable outer membrane consisting of a thick peptidoglycan layer and lipopolysaccharides (LPS) that limit the ability of most antibiotics to penetrate past the cell membrane and reach their intracellular targets (Pang et al., 2019). Additionally, a series of porin channels outline the outer membrane and have a low efficacy for large and/or hydrophobic compounds (thus, antibiotics) and are typically in a closed conformation (Pang et al., 2019; Dreier and Ruggerone, 2015). OprD is a porin within *P. aeruginosa* directly involved in the uptake of basic amino acids and peptides, as well as antibiotics. The absence or reduced expression of this porin channel within *P. aeruginosa* has contributed to reduced antibiotic uptake and an overall increased drug- resistance within the pathogen (Li et al., 2012). Moreover, the outer membrane of *P. aeruginosa* has shown to decrease the net negative charge of the LPS in response to the presence of cationic antibiotics providing effective and adaptable protection (Page, 2012).

Bacterial efflux pumps, specifically the resistance-nodulation-division (RND) family, play an important role in antibiotic resistance of *P. aeruginosa* as well. Efflux pumps are a key mechanism of resistance in Gram-negative bacteria as they expel toxic compounds out of the cell (Soto, 2013). *P. aeruginosa* expresses twelve RND efflux pumps, four of which contribute to antibiotic resistance of quinolone, β-lactam, and aminoglycoside antibiotics (MexAB-OprM, MexCD-OprJ, MexEF-OprN, and MexXY-OprM) (Pang et al., 2019). Overexpression of these efflux systems has been observed in clinical strains of *P. aeruginosa* contributing to multidrug

resistance. While the use of efflux pump inhibitors has been formulated as a therapeutic strategy, this pathogen readily acquires mutations in efflux pump repressors (Braz et al., 2016).

Like most Gram-negative bacteria, *P. aeruginosa* produces antibiotic inactivating enzymes that modify or break down antibiotics, rendering them inactive, as an intrinsic resistance mechanism. The chemical bonds within antibiotics make them susceptible to hydrolysis by enzymes produced by *P. aeruginosa*. For example, β-lactamase is an enzyme encoded by the inducible *ampC* gene and can break the amide bond of the β-lactam ring, while aminoglycoside phosphotransferases (APH) can transfer a phosphoryl group to the 3'- hydroxyl of aminoglycosides thereby inactivating the antibiotics (Wolter and Lister, 2013; Pang et al., 2019). The use of antibiotic inactivating enzymes has contributed to the need of second- or third-line drugs to treat *P. aeruginosa* infections, amplifying the development of MDR pathogens (Burrows et al., 2018).

In addition to the high level of intrinsic resistance *P. aeruginosa* possesses, it readily develops acquired antibiotic resistance mechanisms through mutations (some previously stated) or horizontal gene transfer (Munita and Arias, 2016). As previously mentioned, *P. aeruginosa* readily acquires mutations to modify the expression of specific porins within the outer membrane layer in order to reduce permeability and thereby limit antibiotic penetration. A mutation in the OprD porin specifically confers a high level of resistance to the carbapenem, imipenem (Fang et al., 2014). Out of 61 clinical *P. aeruginosa* isolates resistant to imipenem in Southern China, 50 had frame-shift mutations, premature stop codons, or reduced expression of the OprD porin (Fang et al., 2014; Pang et al., 2019). Mutations that induce conformational changes in the binding or target sites of antibiotics have also contributed to resistance in this pathogen as well as mutations that result in overexpression of the antibiotic-inactivating enzymes. *P. aeruginosa* can

also acquire resistance via mobile genetic elements such as plasmids, transposons, and prophages carrying antibiotic resistance genes. These resistance genes are easily shared between bacteria by conjugation, transduction, or transformation to spread resistance that renders antibiotics ineffective (CDC, 2019; Pang et al., 2019).

Adaptive resistance mechanisms are also highly developed within *P. aeruginosa* that increases its ability to survive even the most toxic environments. It becomes incredibly difficult to treat *P. aeruginosa* infections because it is a prolific developer of antimicrobial- and disinfectant-tolerant communities known as biofilms (Pestrak et al., 2016; Burrows, 2019). Through its aggressive swarming and twitching motilities, it can rapidly spread on most surfaces and colonize regions containing subinhibitory concentrations of antibiotics, forming biofilms even in regions inaccessible to other species (Burrows, 2019). Formation of a biofilm in bacteria is generally more difficult to treat as they consist of an aggregate of microorganisms adhered to each other that are less sensitive to antibacterial agents compared to growing alone (Das et al., 2013). Chronic lung infections by *P. aeruginosa* in CF patients is attributed to the formation of a biofilm; the introduction of an antibiotic to the biofilm induces a stress response for survival under the harsh environment. This further stimulates the formation of persister cells, phenotypic variants that comprise about 1% of biofilm cells and are metabolically inactive, but highly tolerant to antibiotics (Wood et al., 2013). These variants are capable of remaining viable while existing in a dormant state that reduces antibiotic uptake and resuming growth once the antibiotic has been removed (Van den Bergh et al., 2017). Thus, in an MDR strain like *P. aeruginosa*, formation of a biofilm can become fatal, as is usually the case for CF patients.

2.2 Protein Synthesis in Pseudomonas Aeruginosa

Bacterial protein synthesis is a highly dynamic process that comprises of four phases: initiation, elongation, termination, and ribosome recycling (Hu et al., 2016). Structural and functional studies have provided a more in-depth understanding of the mechanisms surrounding the formation of the 30S initiation complex (30S IC). Translation initiation is the most regulated, step-limiting phase mediated by only three initiation factors: IF1, IF2, and IF3. The process of translation requires the presence of mRNA, an aminoacylated and formylated initiator tRNA, and the 70S bacterial ribosome containing an A-, P-, and E-site. IF3 first binds to the small ribosomal subunit (30S) near the E-site to prevent premature binding of the 50S subunit. This is followed by the binding of IF1 to the A-site to ensure availability of the initiator tRNA to the P-site and prevent premature association of the aminoacyl tRNA (Rodnina, 2018). The 30S subunit is then recruited to the ribosome binding site (RBS) on the mRNA through interactions between the Shine-Dalgarno (SD) sequence – if present – of the mRNA and the complementary 16S rRNA of the 30S ribosome, which initiates the binding of IF2 to IF1 on the A-site (Rodnina, 2018). Finally, the initiator fMet-tRNA^{fMet} is recruited to the P-site by GTP-bound IF2, triggering a conformational change in the 30S subunit to create a functionally competent 30S IC (Milon et al., 2012). Formation of the 30S IC is a critical step in the initiation of translation and is often a checkpoint during protein synthesis to ensure fidelity of the entire process (Milon et al., 2012). Once a stable 30S IC is formed, the large ribosomal subunit (50S) will position itself on the 30S ribosome reforming the 70S ribosome, triggering the dissociation of all three initiations factors, and allowing elongation to begin. Each translation factor has multiple, critical roles that regulate the kinetics and fidelity of the overall initiation process (Gualerzi and Pon, 2015).

Currently, there are few antibiotics that target protein synthesis. Streptomycin was the first discovered aminoglycoside antibiotic with bactericidal effects (Luzzatto et al., 1968). Various members of the aminoglycoside family are known to bind the A-site on the 30S ribosome to inhibit protein synthesis with some specificities (Serio et al., 2018). For example, it has been suggested that streptomycin disturbs the movement of ribosomes near the beginning of the mRNA molecules, resulting in inhibition of protein synthesis (Luzzatto et al., 1968). More specifically, formation of the 30S-50S complex is stopped at the starting point and unable to engage in protein synthesis. Moreover, an NMR solution structure revealed the aminoglycoside paromomycin specifically binds an RNA oligonucleotide that contains the 30S subunit A site, allowing the chemical groups of the antibiotic to interact with conserved nucleotides in the RNA, inhibiting the continuation of protein synthesis (Fourmy et al., 1996). Another aminoglycoside antibiotic, gentamicin, can enter through the Gram-negative membrane in oxygen dependent active transport and bind the 16S rRNA at the 30S subunit, disturbing the translation of mRNA and leading to the formation of truncated or nonfunctional proteins (Beganovic et al., 2018). Lastly, tetracycline antibiotics are believed to inhibit translation by binding to the 16S rRNA and inhibiting the binding of aminoacyl-tRNA to the mRNA-ribosome complex (Chopra and Roberts, 2001). Unfortunately, most of these antibiotics are broad-spectrum antibiotics and not specific enough to inhibit MDR strains. The elucidation of 3D atomic-level structures of proteins in species-specific protein synthesis is required for more narrow-spectrum, specific, antibiotics.

2.2.1 Translation Initiation Factors

Several structures of the initiation factor 1 (IF1) in bacteria have been elucidated either in free form or bound to the 30S subunit (Sette et al., 1997; Hu et al., 2016). IF1 is the smallest of the initiation factors containing 71 amino acid residues that make up a 5 stranded β-barrel protein containing a single domain, a short α-helix, and an oligo-binding fold (Milon nd Rodnina, 2012; Hu et al., 2016). The binding of IF1 is known to stabilize the binding and enhance the activities of IF2 and IF3, creating a more stabilized 30S pre-initiation complex (PIC) (Milon and Rodnina, 2012; Mion et al., 2012; Rodnina, 2018). Crystal structures of IF1 in *E. coli* have suggested that it promotes the displacement of the h44 strand on the 30S subunit, suggesting that IF1 actively remodels the 16S rRNA to modulate the confirmation of the 30S subunit during binding of the mRNA (Qin et al., 2012; Milon and Rodnina, 2012). Moreover, studies that have interfered with the conformational mobility of the 30S ribosome or omitted IF1 entirely have seen a reduced fidelity of the initiation process (Milon and Rodnina, 2012).

As previously mentioned, in *P. aeruginosa* PaIF1 is the smallest initiation factor containing a 5-stranded β-sheet that adopts a β-barrel fold with an OB motif (Milon and Rodnina, 2012; Hu et al., 2016). The full-length solution NMR structure of PaIF1 was previously elucidated and the sequential order of the PaIF1 protein observed was: β1-β2-β3-α1- β4-β5 (Hu et al., 2016). An alignment of the primary sequence of PaIF1 with that of bacterial homologs *E. coli, Mycobacterium tuberculosis, Streptococcus pneumoniae, Burkholderia thailandensis*, and *Thermus thermophilus* revealed that these structures are highly similar and multiple residues are highly conserved with significant differences noted in the C- terminal region (Hu et al., 2016). Indeed, the amino acid sequence of PaIF1 is most similar to that of IF1 from *E. coli;* however, PaIF1 contains an unusually extended β-strand at the C- terminal domain that is more rigid

compared to the C-terminal domain of EcIF1 (Hu et al., 2016). Interestingly, residues near the C-terminal end have shown to be most critical for IF1 functionality, thus the structural differences observed in each species may explain individual interactions with their cognate 30S ribosome (Hu et al., 2016). Moreover, surface properties of IF1 revealed the β-strands near the α-helix is rich in basic residues like Arg and Lys (Hu et al., 2016). These residues were observed to be highly conserved in other bacterial IF1 proteins and shown to be involved in binding to the 30S ribosomal subunit in the crystal structure of IF1 from *T. thermophilus* (Carter et al., 2001; Hu et al., 2016).

IF3 is made up of a C- and N-terminal domain connected by a hydrophilic, lysine-rich linker (Julian et al., 2011; Li et al., 2020). IF3 enhances the fidelity and speed of the initiation process and contains multiple dynamic roles during the initiation of translation. The initiation factor undergoes large conformational changes that require extensive flexibility (Hussain et al., 2016; Nakamoto et al., 2021). Fluorescence data suggests that IF3 fluctuates between a closed and an open conformation, with the open conformation being more stable once IF3 has bound to the 30S subunit (Milon and Rodnina, 2012). A high-resolution structure of each domain individually has been elucidated in *E. coli*, and dynamic analyses have shown that each terminal domain can occupy up to two binding sites on the 30S subunit independently of each other (Nakamoto et al., 2021). Cryo-EM analyses have noted that the C-terminal domain of IF3 interacts with the 790 loop of 16S rRNA, while the N-terminal domain is in close proximity to the formylated initiator tRNA, fMet-tRNA^{fMet} (Julian et al., 2011). The N-terminal domain has also been seen to interact with the 30S platform, while the C-terminal domain interacts with the P site of the 30S ribosome. Interestingly, a mutation induced in the N-terminal region of IF3 allowed the initiation factor to bind the 30S ribosome normally, but the fidelity of fMet-tRNA

selection was affected (Maar et al., 2008). Cryo-EM structures with and without IF3 have also noted a conformational rearrangement of the 30S subunit; upon binding of IF3, the 30S subunit is seen to rotate into the position seen in the 70S ribosome, whereas in the absence of IF3, the small ribosomal subunit is in its classic 30S structure (Simmonetti et al., 2008; Julian et al., 2011). As previously mentioned, the most noted role of IF3 involves binding to the 30S subunit to prevent premature association of the 50S subunit. Additional roles of IF3 previously observed in *E. coli* include discriminating against mRNAs with unfavorable translation initiation regions and ensuring the appropriate initiator tRNA, fMet-tRNA^{fMet}, is selected for translation initiation (Milon and Rodnina, 2012; Rodnina, 2018).

While individual domains have been found, a high-resolution, full-length structure of IF3 has not been elucidated, making it difficult to understand the precise dynamic interactions of this protein with the 30S subunit, such as which specific amino acids are required for binding. Moreover, the interplay of each terminal domain with each other and independently of each other is unknown. Previously, the NMR resonance assignments of IF3 in *P. aeruginosa* were explained as an initial step in understanding the mechanism of interaction with the 30S subunit and protein synthesis in this pathogen (Li et al., 2020). From the NMR chemical shift data, secondary structure analyses presumed nine β-strands and four α-helices arranged in the following order: β1-β2-α1-β3-β4-α2-β5-α3-β6-α4-β7-β8-β9 (Li et al., 2020). Additionally, the lowest energy structure of the C-terminal domain of IF3 in *P. aeruginosa* has been reported in the Protein Data Bank (PDB), supporting the previously obtained NMR resonance assignments (**PDB: 6VRJ; Figure 1**).

NMR titration of PaIF1 with the 30S ribosome revealed the region containing the most significant perturbation was the short α-helix containing residues His-35, Ile-36, Gly-38, Arg-41,

Tyr-44, and Leu-48 as shown in **Figure 2** (Hu et al., 2016). A structural model of IF1 with the 30S ribosome also revealed that the α-helical region anchors IF1 to the A site during protein synthesis. Based on these previously obtained results, a PaIF1 peptide was derived from the α-helix in IF1 to be utilized as a functional mimic. We hypothesized that the peptide could compete with IF1 for binding to the 30S subunit thereby inhibiting protein synthesis in *P. aeruginosa*, and ultimately inhibiting bacterial growth. The PaIF1 peptide and the elucidation of the C-terminal domain in PaIF3 was utilized to address the following aims: (1) determine the regulations of translation initiation factor 1 in *P. aeruginosa* and (2) elucidate a high-resolution NMR structure of translation initiation factor 3 (PaIF3).

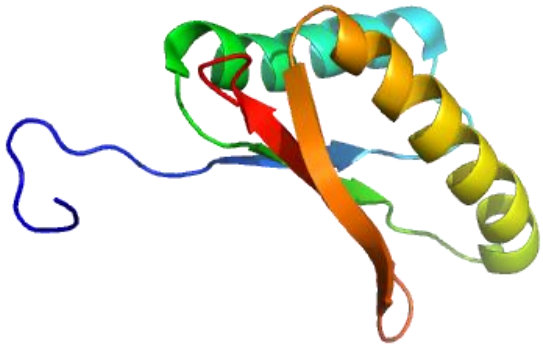

Figure 1. High-resolution structure of IF3C domain in *P. aeruginosa* (PDB 6VRJ).

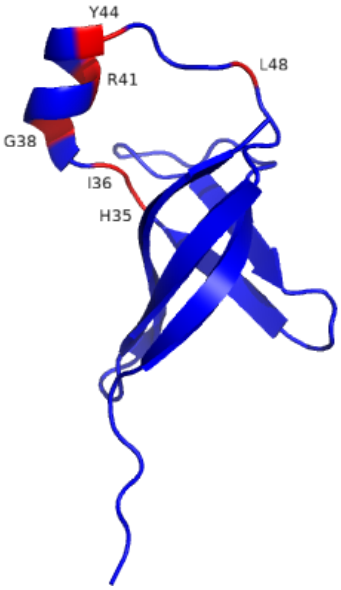

Figure 2. High-resolution structure of initiation factor 1 in *P. aeruginosa*. Amino acid residues observed to have the most significant perturbation when bound to the 30S ribosome labeled using PyMOL (PDB 2N78).

2.3 Antimicrobial Peptides

The exhaustion of the antibiotic pipeline has resulted in the search for alternatives to combat bacterial infections. Antimicrobial peptides (AMP) have increasingly been suggested as an alternative to conventional antibiotics based on their broad-spectrum activity (Pang et al., 2019). AMPs are a diverse group of bioactive small proteins and have been a line of defense for a variety of organisms against pathogenic bacteria for many years as they originated from host defense peptides that belong to the innate immune system (Magana et al., 2020; Liu et al., 2021). Different from antibiotics, AMPs are typically less than 100 residues that often consist of positively charged amino acids such as arginine, lysine, and histidine (Browne et al., 2020). Due to their composition, AMPs are typically considered cationic, or positively charged; thereby enabling them to interact with the negatively charged components of bacterial cell membranes (Browne et al., 2020; Liu et al., 2021). The most common mechanism of action of AMPs is to

penetrate and disrupt the bacterial cell membrane resulting in the formation of pores or the breakdown of membrane potential and permeability as well as metabolite leaking and ultimately, bacterial cell death (Pushpanathan et al., 2013; Lee et al., 2016; Browne et al., 2020). However, their structural, chemical, and functional diversity makes it difficult to define a specific mode of action as most AMPs possess multiple targets.

Their small size contributes to their ability to rapidly diffuse throughout the cell and exhibit a rapid defensive response against pathogenic microbes compared to current antibiotics. Some AMPs have been noted to interact with intracellular targets such as DNA, RNA, and protein synthesis (Liu et al., 2021). Specific AMPs rich in proline residues, such as pyrrhocoricin and drosocin, were proposed to penetrate the cellular membrane and inhibit the ATPase activity of the heat-shock protein DnaK and the chaperon GroEL, disrupting adequate protein folding (Kragol et al., 2001; Liu et al., 2021). Additionally, some AMPs can bind to the negatively charged phosphate groups of the lipopolysaccharide (LPS) layer in Gram-negative bacterial membranes by displacing cations such as Ca^{+} and Mg^{2+}, important nutrients required by bacteria for growth and cell maintenance (Liu et al., 2021). The secondary structures of AMPs have been classified into four groups: α-helical, β-sheet, a hybrid of both, and peptides with a random/extended structure (Liu et al., 2021). Majority of AMPs exhibit α-helical structures such as Spinigerin, a cysteine-lacking antimicrobial that interacts with trypanothione reductase, reducing its ability to detoxify the cell of reactive oxygen species (ROS) targets (Sardar et al., 2013).

The ability for AMPs to induce bacterial cell death via multiple mechanisms and non-specific targets reduces the likelihood of pathogens to produce resistance (Browne et al., 2020; Liu et al., 2021). Moreover, organisms can produce more than one AMP, further reducing the

chance of resistance. Additionally, the ability of a single antimicrobial peptide with multiple mechanisms to induce bacterial cell death may present less side effects compared to the combination of multiple antibiotics.

Currently there are very few commercially available AMPs such as Gramicidin D, Dalbavancin, and Colistin, all of which are associated with the disruption of bacterial cell membranes directly or indirectly (Browne et al., 2020). Additionally, there is a gap in the market for compounds effective against Gram-negative bacteria, or the ESKAPE pathogens (*Enterococcus faecium, Staphylococcus aureus, Klebsiella pneumoniae, Acinetobacter baumannii, Pseudomonas aeruginosa,* and *Enterobacter spp.),* four of which are Gram-negative and have been deemed a priority pathogen by the World Health Organization (De Oliveira et al., 2020). The development of synthetic peptides, specifically protein mimics, has become a promising topic. Apart from expanding the chemical and structural diversity of peptides, the ability to design and optimize a peptide mimic can ultimately introduce new mechanisms of action and increase the half-life of a peptide and/or its proteolytic stability. Moreover, synthetic peptides can be generated as an exact copy of their cellular targets, thereby enhancing their antimicrobial abilities and biological applications (Gro et al., 2016).

CHAPTER III

METHODOLOGY AND FINDINGS

3.1 Methodology

3.1.1 Sequence Alignments

FASTA sequences of the primary sequence of IF1 and IF3 structures from *P. aeruginosa* and bacterial homologs (*E. coli, Mycobacterium tuberculosis, Streptococcus pneumoniae, Burkholderia thailandensis,* and *Thermus thermophilus*) were obtained from the National Center for Biotechnology Informaton (NCBI) Genbank sequence database and submitted to the ClustalOmega Multiple Sequence Alignment (MSA) tool data resource. Only *E. coli, M. tuberculosis,* and *S. pneumoniae* were used in the sequence alignment of IF3.

3.1.2 PaIF1 Peptide

The peptide (NH_2-AHISGKMRKNYIRILTG-COOH) derived from the short α-helix in IF1 was obtained from Apeptide Co. Ltd. (China). The peptide was chemically synthesized and purified using HPLC purification with a SinoChrom ODS-BP (5 *u*m, 250 x 4.60 mm) column. The peptide was eluted using a gradient of buffer A (0.1 trifluoroacetic acid in 100% acetonitrile) and B (0.1% trifluoroacetic acid in 100% water) with a flow rate of 1 mL/min as a single peak via HPLC with >95% purity (Valdez et al., 2021). The peptide was verified using ESI-MS

(SHIMADZU LCMS-2010EW) with an experimental value (1958.38) close to the theoretical mass (195.36) as described previously in Valdez et al. (2021).

3.1.3 Microbiological Assay

Antimicrobial activity of the PaIF1 peptide was investigated using Thermo Fisher Scientific 96-Well Microtiter Microplates via a Minimum Inhibitory Concentration assay (MIC). The representative bacteria for the assay included *P. aeruginosa* (ATCC 47085), *Escherichia coli* (One Shot BL21 (DE3), cat. No. C600003) from Invitrogen, *Staphylococcus epidermitis* (ATCC 12228), *Mycobacterium smegmatis* (ATCC 14468), *Bacillus cereus* (ATCC 14579), *Alcaligens faecalis* and *Proteus vulgarius*, both obtained from The Microbiology Laboratory, University of Texas Rio Grande Valley. All bacterial cultures were grown overnight at 37°C on LB or Nutrient Agar (dependent on the growth conditions observed to produce maximum bacterial growth; Table 1.0) from stock. About 5-6 colonies were inoculated into 20mL LB or Nutrient broth and grown at 37°C, 200 rpms to an Optical Density (OD_{600}) of 0.08-0.13. The Microtiter plate was set up by adding 50uL of the bacterial culture into each well containing varying concentrations of the PaIF1 peptide, DMSO (negative control), or ampicillin and/or kanamycin (positive controls). The PaIF1 peptide was diluted by a series of 2-fold dilutions from the first well across the plate resulting in a concentration range of 3.0 mg/mL to 0.0 mg/mL; each assay was performed in triplicate. The Microtiter plate was incubated overnight at 37°C. The first well with no growth was considered the MIC.

3.1.4 Swarming Assay

Overnight cultures of *P. aeruginosa* strain PAO1 (ATCC 47085) were grown on LB agar media overnight at 37°C. About 2-4 colonies were inoculated into 5mL of LB broth and grown at 37°C, 225 rpm. When the OD_{600} reached ~1.0, 1uL of bacterial culture was inoculated onto the center of a cooled swarming medium and incubated for 24h at 30°C. The swarming medium consisted of a Modified M9 Minimal medium (20 mM NH_4Cl, 12 mM Na_2HPO_4, 22 mM KH_2PO_4, 8.6 mM NaCl, 1 mM $MgSO_4$, 1 mM $CaCl_2$ $2H_2O$, 11 mM dextrose, and 0.5% Agar) with varying concentrations of the PaIF1 peptide (30 mg/mL) cooled for exactly 60 min as described (Jiang et al., 2020).

3.1.5 Cytotoxicity Assay of PaIF1 Peptide

To observe the toxic effect, if any, of the PaIF1 peptide on human cell cultures, human embryonic kidney cells (HEK-293) in Dulbecco's modified Eagle's medium (DMEM) with 10% Fetal Bovine serum (FBS) and Penicillin-Streptomycin solution were plated in 96-well plates with 25,000 cells per well (Valdez et al., 2021). The plates were incubated in a CO_2 incubator with 5% CO_2 at 37°C for 18 hours. Cells were treated with the peptide, which was previously dissolved in DMSO and diluted to yield a final concentration from 3 mg/ml to 1 ug/ml, or dichlorodiphenyltrichloroethane (DTT) as a positive control, or DMSO as a negative control and incubated for another 18h. The Trevigen TACS MTT Cell Proliferation Assay Kit (Gaithersburg, MD) was utilized to assess the impacts of the PaIF1 peptide on human cell proliferation and/or viability. MTT reagent (10ul) was added to each well and incubated under 5% CO_2 at 37°C for another 4h. Lastly, 100ul of detergent reagent was added to each well and incubation was continued overnight. Samples were conducted in double.

3.1.6 Predicted Protein Structures

The solution NMR structures of the PaIF1 peptide, PaIF3N, PaIF3NΔ20, and a full-length structure of PaIF3 were predicted by using the trRosetta server available at https://yanglab.nankai.edu.cn/trRosetta/. The protein structures were predicted with an estimated TM-score of 0.333, 0.834, 0.865, and 0.725, respectively.

3.1.7 Expression and Purification of PaIF3N

Previously, the gene encoding the N-terminal of translation initiation factor 3 in *P. aeruginosa* was inserted into the pET-24b(+) vector (Novagen) using NheI and XhoI restriction enzymes in our lab. The resultant protein contained two amino acids (AS) between the start codon and the body of the protein at the N-terminus, while a His-tag (LEHHHHHH) was inserted at the C-terminal for the purpose of purification (Li et al., 2020). The recombinant plasmid was transformed into Rosetta 2(DE3) *E. coli* competent cells (Novagen). Overnight cultures of *E. coli* cells harboring the pET24b PaIF3N plasmids (10mL) were added to 1L of fresh M9 Minimal Medium containing 1 g/L of $^{15}NH_4Cl$ for a uniformly ^{15}N-labeled PaIF3N protein and kanamycin (0.1 g/ml). Bacteria were grown at 37°C, shaking at 225-250 rpms to an OD_{600} of 0.8-1.0. Overexpression of the target protein was induced by isopropyl β-D-1-thiogalactopyranoside (IPTG) to a final concentration of 0.5 mM. After 4 hours of postinduction incubation, the bacterial cells were collected by centrifugation (6000 rpm, 4°C, 15 min). The cell pellets were resuspended in a His-tag binding buffer solution with phenylmethylsulfonyl fluoride (PMSF) and dithiothreitol (DTT) and sonicated to produce a cell lysate. The cellular components were harvested by centrifugation at 18,000 rpm for 1 hour at 4°C. Following centrifugation, the supernatant from the cell lysate was loaded onto a Ni-affinity column to purify the protein of

interest using nickel-nitrilotriacetic acid affinity chromatography (Ni-NTA) and allow the His-tag of PaIF3N to bind the nickel in NTA beads. After column washing to remove impurities, PaIF3N was eluted by a 500 mM imidazole containing buffer. The purified PaIF3N protein underwent dialysis to remove high salts for buffer exchange. The His-tagged PaIF3N protein was purified to >98% homogeneity with a molecular weight of 9.5 kDa as determined by sodium dodecyl-sulfate polyacrylamide gel electrophoresis (SDS-PAGE).

3.1.8 NMR Spectroscopy

^{15}N-labeled PaIF3N purified proteins were exchanged into a buffer containing 25 mM phosphate (pH 6.5), 25mM NaCl, DTT, and 8% D_2O using a Millipore Amicon Ultra Centrifugal Filter *Ultracel-3K* (Millipore #UFC900324, 3 kDa cut-off) and concentrated to about 1.0 mM. Protein samples were centrifuged for 10 minutes at 13.4k rpms to remove any precipitates and transferred to NMR Shigemi tubes. NMR data was collected at 298K on a Bruker Ultrashield Plus 600 MHz spectrometer equipped with a double resonance broad band room-temperature probe (BBO), or a Bruker Avance 700 MHz or 600 MHz spectrometer both equipped with a four-channel interface and triple resonance cryogenic probes (TCI) with single-axis (Z) pulse field gradients. The ^{15}N-^{1}H HSQC spectrum was recorded using a sample of ^{15}N-labeled PaIF3NΔ20 with 256 (F1) x 1024 (F2) complex points. Backbone and side-chain NMR chemical shift assignments were obtained by analyzing the following spectra: HNCACB, CBCA(CO)NH, HNCO, HBHA(CO)NH, (H)CC(CO)NH, H(CC)(CO)NH, and ^{15}N-HSQC-TOCSY. The ^{13}C-CT-HSQC and ^{13}C-HCCH-TOCSY spectra were used to assign additional side-chain aliphatic ^{1}H and ^{13}C resonances. For aromatic side-chain chemical shift assignments, ^{13}C-CT-HSQC-TOCSY, ^{13}C-HSQC-NOESY spectra along with 2D ^{1}H-^{1}H NOESY and TOCSY were used.

3.1.9 Recombinant Plasmid Construction, Expression and Purification of PaIF3NΔ20

A forward primer with a 20 amino acid deletion (PaIF3NΔ20) at the N-terminal was designed with the NheI restriction enzyme (5'-ggctagcgagaacatctcggctctgag-3'). The 240-245 bp DNA fragment encoding the truncated N-terminal domain of *P. aeruginosa* IF3 (PaIF3 N-domain, ~70 amino acids) was amplified by polymerase chain reaction (PCR). The PCR product was inserted into the pET24b(+) vector (Novagen) between the NheI and XhoI restriction site to construct a plasmid of pET24b PaIF3NΔ20 containing three extra amino acids (MAS) at the N-terminus and a C-terminal six histadine tag (LEHHHHHH). The recombinant plasmid, confirmed via DNA sequencing, was transformed into One Shot® BL21(DE3) *E. coli* competent cells (Invitrogen). For uniformly ^{15}N-labeled PaIF3NΔ20 overexpression, 10mL overnight culture of LB medium with BL21(DE3) cells harboring pET24b PaIF3NΔ20 plasmids were added to M9 Minimal Medium containing 1 g/L of $^{15}NH_4Cl$ and kanamycin (0.1 g/mL). Bacterial cell cultures were grown at 37°C, shaking at 225-250 rpms to an OD_{600} of 0.8-1.0. Overexpression of the target protein was induced by isopropyl β-D-1-thiogalactopyranoside (IPTG) to a final concentration of 0.5 mM. After 4h of postinduction incubation, the bacterial cells were collected by centrifugation (6000 rpm, 4°C, 15 min). The cell pellets were resuspended in a His-tag binding buffer solution with phenylmethylsulfonyl fluoride (PMSF) and dithiothreitol (DTT) and sonicated to produce a cell lysate. The cellular components were harvested by centrifugation at 18,000 rpm for 1 hour at 4°C. Following centrifugation, the supernatant from the cell lysate was loaded onto a Ni-affinity column to purify the protein of interest using nickel-nitrilotriacetic acid affinity chromatography (Ni-NTA) and allow the His-tag of PaIF3NΔ20 to bind the nickel in NTA beads. After column washing to remove impurities,

PaIF3NΔ20 was eluted by 500 mM imidazole containing buffer. The purified PaIF3NΔ20 protein underwent dialysis to remove high salts for buffer exchange.

3.1.10 NMR Spectroscopy of PaIF3NΔ20

^{15}N-labeled PaIF3NΔ20 purified proteins were exchanged into a buffer containing 25 mM potassium phosphate (pH 6.5) and 5mM DTT using a Millipore Amicon Ultra Centrifugal Filter *Ultracel-3K* (Millipore #UFC900324, 3 kDa cut-off) and concentrated to about 1.0 mM. Protein samples were centrifuged for 10 minutes at 13.4k rpms to remove any precipitates and transferred to NMR Shigemi tubes with 8% D_2O. All NMR experiments were performed at 298K on a Bruker Ultrashield Plus 600 MHz spectrometer equipped with a double resonance broad band room-temperature probe (BBO), or a Bruker Avance 700 MHz or 600 MHz spectrometer both equipped with a four-channel interface and triple resonance cryogenic probes (TCI) with single-axis (Z) pulse field gradients. The ^{15}N-^{1}H HSQC spectrum (Figure #) was recorded using a sample of ^{15}N-labeled PaIF3NΔ20 with 256 (F1) x 1024 (F2) complex points. Backbone and side-chain NMR chemical shift assignments were obtained by analyzing the following spectra: HNCACB, CBCA(CO)NH, HNCO, HBHA(CO)NH, (H)CC(CO)NH, H(CC)(CO)NH, and ^{15}N-HSQC-TOCSY. The ^{13}C-CT-HSQC and ^{13}C-HCCH-TOCSY spectra were used to assign additional side-chain aliphatic ^{1}H and ^{13}C resonances. For aromatic side-chain chemical shift assignments, ^{13}C-CT-HSQC-TOCSY, ^{13}C-HSQC-NOESY spectra along with 2D ^{1}H-^{1}H NOESY and TOCSY were used.

3.2 Findings

3.2.1 Regulations of Translation Initiation Factor 1 in *P. aeruginosa*

Previously, the full-length solution NMR structure of IF1 in *P. aeruginosa* was elucidated in our lab (Hu et al., 2016). Surface properties of IF1 revealed that two β-strands near the α-helix is rich in basic residues, such as Arg and Lys (Hu et al., 2016). Interestingly, the sequence alignment of IF1 in *P. aeruginosa* and other bacterial homologs revealed a series of highly conserved residues, particularly Arg and Lys residues as shown in **Figure 3**. Additionally, a series of residues (outlined in red) near the second β-sheet and short α-helix are highly conserved in all homologs, indicating this may a functionally important region within the protein. Although the secondary structures are highly similar, there are significant differences in the C-terminal regions. Multiple amino acids, specifically Arg70 were found to be critical for IF1 functionality in *E. coli*; however, in the crystal structure of IF1 from *T. thermophilus* (PDB: 1HR0), Arg70 makes no direct contact with the 30S ribosome suggesting that initiation factors from distinct species may exhibit individualized binding characteristics with the 30S ribosomal subunit (Sette et al., 1997; Hu et al., 2016).

We decided to test the PaIF1 peptide against a range of pathogenic and non-pathogenic bacterial species, including Gram-negative and Gram-positive strains (Table 1.0). Compared to negative (DMSO) and positive (ampicillin and kanamycin) controls, the PaIF1 peptide exhibited inhibitory activity against all seven bacteria tested (**Figure 4**). Bacterial growth in *P. aeruginosa* was most inhibited with the lowest MIC of 0.047 mg/mL. The MICs of *E. coli* and *A. faecalis* was 0.15 mg/mL. Against *P. vulgaris* the PaIF1 peptide exhibited a MIC of 2.1 mg/ml, while a MIC of 0.75 mg/mL was exhibited against *S. epidermitis* and *M. smegmatis*. Lastly, the peptide exhibited a MIC of 1.5 mg/mL against *B. cereus*. Interestingly, compared to ampicillin – a

commonly used broad-spectrum antibiotic, the PaIF1 peptide exhibited better inhibitory activity against *P. aeruginosa, A. faecalis, M. smegmatis, and B. cereus* (**Fig. 4C-D and 4F-G**). Nonetheless, the MIC values compared to *in vitro* assays, suggests the binding of the PaIF1 peptide is weaker compared to IF1 (Valdez et al., 2021). As such, its antimicrobial potency requires further improvement, optimization, and analysis.

A highly developed quorum sensing system within *P. aeruginosa* regulates a critical virulence factor known as swarming. Swarming is a complex form of motility that allows bacteria to rapidly colonize new surfaces and increases the spread of infections. Additionally, it has shown to result in an increased production of virulence factors and antibiotic resistance (Overhage et al., 2008). Moreover, swarming cells have exhibited an adaptive resistance response against gentamicin, ciprofloxacin and polymyxin B (Overhage et al., 2008). Therefore, the PaIF1 peptide was tested against *P. aeruginosa* PAO1 (ATCC 47085) for its effects on swarming motility. Compared to the control (blank) agar plate, there was a visible reduction in growth and/or swarming of *P. aeruginosa* (**Figure 5**). Additionally, there was an increase in growth when the peptide concentration was reduced from .018 mg/ml to .015 mg/ml, while the increase in concentration from .015 mg/ml to .03 mg/ml shows a reduced amount of swarming, indicating that the PaIF1 peptide may inhibit swarming in *P. aeruginosa* (**Figure 5B**). Overall, the inhibitory effect of the peptide on swarming may be concentration dependent.

While the PaIF1 peptide exhibits antimicrobial activity against a series of bacteria and may reduce the effects of swarming, we wanted to ensure its activity was effective without damaging the host. Human embryonic kidney cells (HEK-293) were incubated with the PaIF1 peptide to assess the qualitative metabolic activity of the cells (**Figure 6**). As expected, DMSO did not inhibit HEK-293 cells at any concentration; however, DTT began to affect the cellular

metabolic activity of the cells at 0.75 mg/ml to the highest concentration of 3.0 mg/ml. The PaIF1 peptide exhibited less viable cells between 0.375 and 1.5. mg/ml, but only entirely inhibited cells at 3.0 mg/ml (**Figure 6**). Most interestingly, the PaIF1 peptide did not affect the metabolic activity of HEK-293 cells at 0.047 mg/ml, which was the MIC of the peptide in *P. aeruginosa*. Based on these results, it can be expected that the peptide can inhibit bacterial growth without providing damage to the host at the respective MIC for *P. aeruginosa*.

To ensure the isolated α-helical region is as expected and its structure-function relationship has not been disturbed, it is important to obtain a high-resolution NMR solution structure. The predicted structure of the PaIF1 peptide by trRosetta reveals an α-helical structure as expected with differences in the unstructured, or flexible, regions of the protein, such as the region containing residues H35, I36, and L48 (**Figure 7A**). Additionally, the overlay of the IF1 peptide predicted structure with IF1 in *P. aeruginosa* displays a shortened α-helical coil on each end (**Figure 7B**). Overall, the obtained structure of the peptide requires optimization via NMR chemical shift assignments.

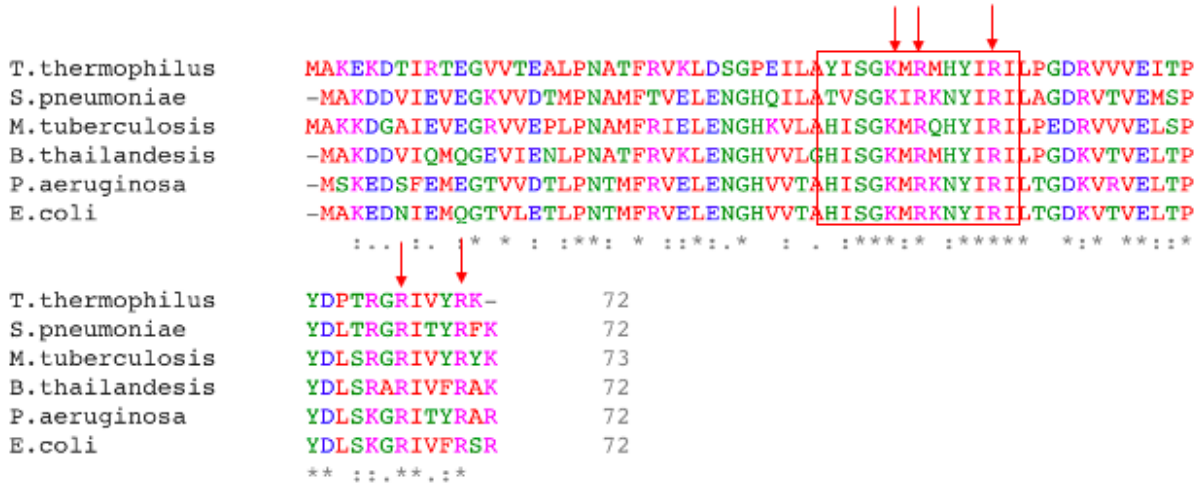

Figure 3. Sequence alignment (ClustalOmega) of IF1 in *P. aeruginosa.* Sequence aligned with those of bacterial homologs *E. coli* (PDB 1AH9), *M. tuberculosis* (PDB 3I4O), *S. pneumoniae* (PDB 4QL5), *B. thailandensis* (PDB 2N3S), and *T. thermophilus* (PDB 1HR0). Residues with arrows represent the conserved Arg and Lys residues; residues outlined in red are conserved in all homologs.

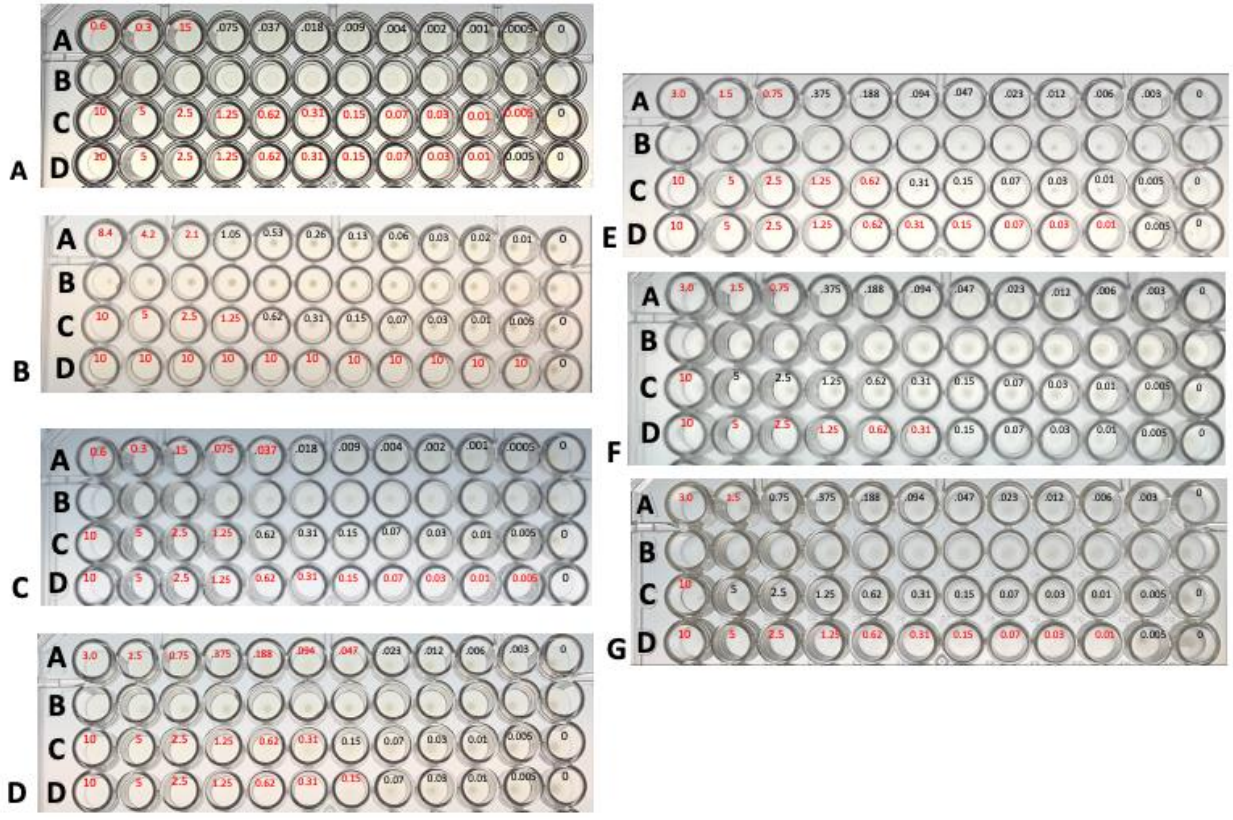

Figure 4. Minimum Inhibitory Concentration (MIC) Assays. Tested against (A) *E. coli*, (B) *P. vulgaris*, (C) *A. faecalis*, (D) *P. aeruginosa*, (E) *S. epidermidis*, (F) *M. smegmatis*, and (G) *B. cereus.* For each figure Row A contains the target bacteria, Row B contains the DMSO negative control, Row C contains ampicillin, and Row D contains kanamycin. Respective growth conditions in Table 1.0. All values in mg/ml.

Table 1.0 Summary of each strain, growth conditions used, stock concentration of the PaIF1 peptide, and their respective MIC (mg/mL).

Species Name	Strain	Media*	Peptide Stock	MIC (mg/ml)
Escherichia coli	BL21(DE3)	LB agar/broth	6 mg/ml	.15
Alcaligens faecalis	Microbiology Laboratory, UTRGV	LB agar/broth	6 mg/ml	.15
Proteus vulgaris	Microbiology Laboratory, UTRGV	LB agar/broth	28 mg/ml	2.1
Pseudomonas aeruginosa	ATCC 47085	LB agar/broth	30 mg/ml	.047
Staphylococcus epidermitis	ATCC 12228	Nutrient agar/broth	30 mg/ml	1.5
Mycobacterium smegmatis	ATCC 14468	LB agar/broth	30 mg/ml	.75
Bacillus cereus	ATCC 14579	Nutrient agar/broth	30 mg/ml	1.5

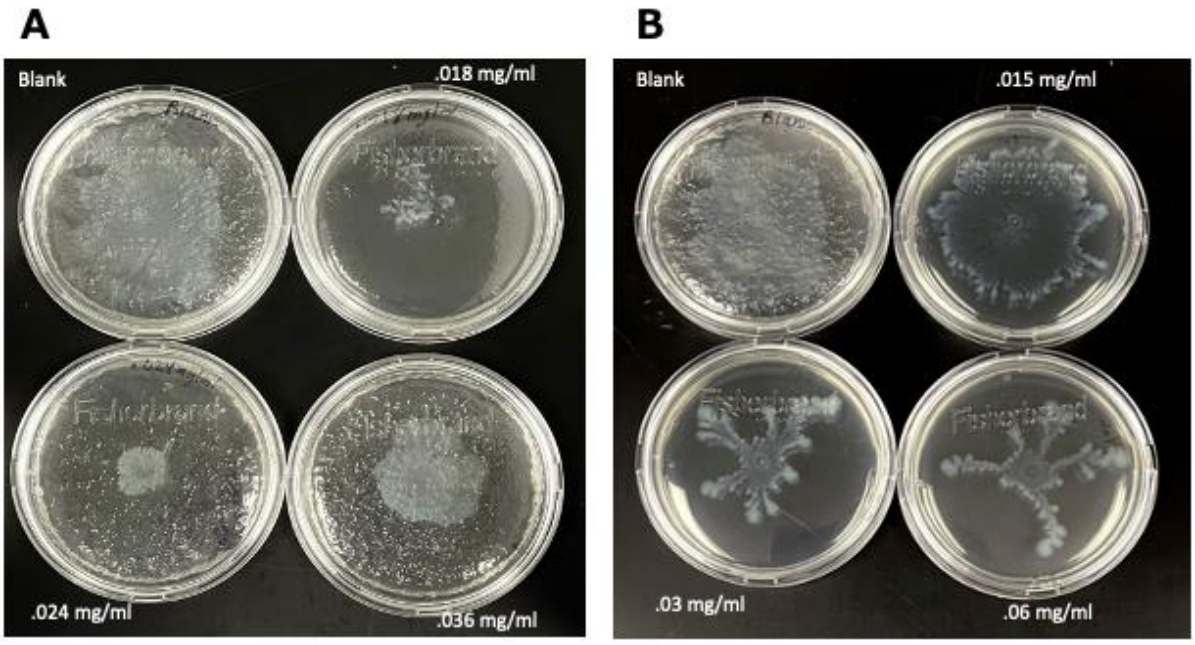

Figure 5. Swarming assay of PaIF1 peptide against *P. aeruginosa* PAO1. (A) First test against swarming at concentrations lower than the MIC: .018 mg/ml, .024 mg/ml, and .036 mg/ml. This test was done in triplicate. (B) Second test against swarming with increased concentrations of the PaIF1 peptide to observe a larger difference in growth.

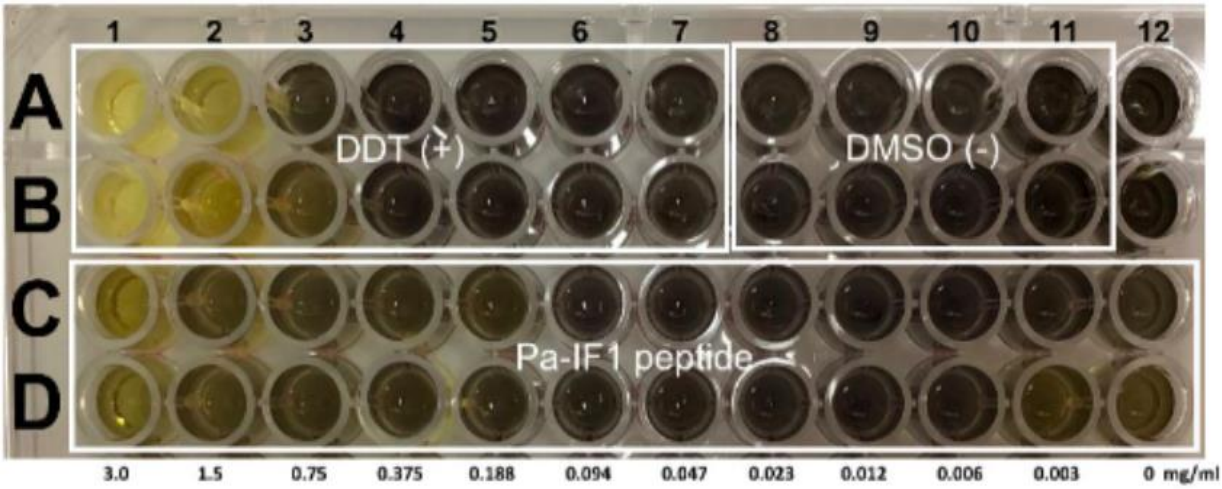

Figure 6. Cytotoxicity effects of the PaIF1 Peptide. Cytotoxicity test done using HEK-293 cells using the Trevigen TACS MTT Cell Proliferation Assay. Each assay was done in double as shown. DMSO and DDT were used as negative and positive controls, respectively.

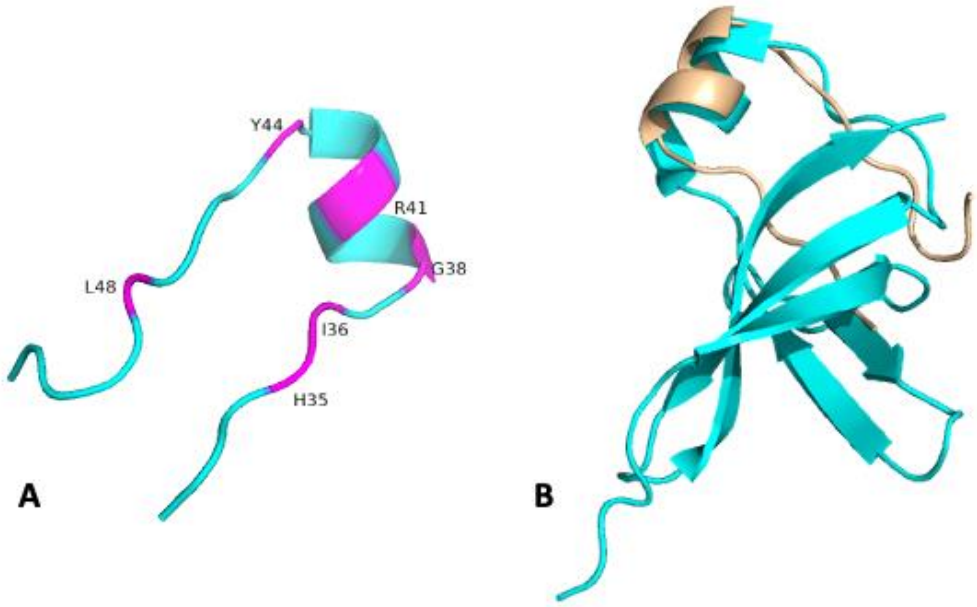

Figure 7. Predicted structure of the PaIF1 peptide. (A) Predicted structure of the PaIF1 peptide in cyan with amino acid residues with most significant perturbations during NMR titration with the 30S subunit in magenta. Estimated TM-score of 0.333. Data obtained from the trRosetta server and labeled using PyMOL. (B) Overlay of the predicted peptide structure (wheat) with IF1 in *P. aeruginosa* (cyan). Data obtained using PyMOL.

3.2.2 Elucidation of A High-Resolution NMR Structure of Translation Initiation Factor 3

It has been proposed that the domains of IF3 bind to the 30S subunit independently, with the C-terminal domain binding first followed by the N-domain. Moreover, most of the functions of IF3 have been attributed to the C-domain by in vitro studies and knockout studies of IF3 have implicated that the C-domain is required for survival while the N-domain may not be (Ayyub et al., 2017). However, in the absence of the N-domain, bacterial growth and fidelity of initiation of protein synthesis is compromised (Ayyub et al., 2017). The sequence alignment of IF3 in *P. aeruginosa* with bacterial homologs reveals a series of highly conserved residues, more specifically in the N-terminal region (**Figure 8**), supporting the indication that amino acid residues present in the N-terminal region may be important for the fidelity of protein synthesis in bacteria. Additionally, a study by Maar et al. revealed that a substitution mutation of Tyr-75 to Asn-75 in the N-terminal domain of EcIF3 perturbs the fidelity of the translation initiation process (2008). The mutated domain of IF3 reduced its ability to discriminate between start-codons and select initiator tRNAs (Maar et al., 2008). Residue 75 in *E. coli* and *M. tuberculosis* are similar (Tyr), while residue 75 in *P. aeruginosa* and *S. pneumoniae* are similar (Phe), further supporting the idea that highly similar amino acids in each bacterium are required for the fidelity of species-specific protein synthesis.

To obtain a full-length solution structure of IF3, we proposed that, due to the high flexibility of interdomain linker and overall structure of IF3, the individual domains should be studied and clarified individually. As previously mentioned, the IF3C domain has been elucidated in our lab (PDB 6VRJ). Therefore, the focus of this study was the elucidation of the IF3N domain. The predicted structure of IF3N is shown in **Figure 9**. The best predicted structure shows an unstructured region within the first 20 amino acid residues of the protein in orange with

four β-strands and one α-helix. It was proposed that this region contributed to high flexibility of the N-domain and resulted in a series of signal overlaps and an inconclusive 3D NMR structure of the N-terminal region in PaIF3. Thus, we theorized that the first 20 amino acid residues in the N-terminus may not be used functionally in PaIF3.

The two-dimensional ^{1}H, ^{15}N heteronuclear single quantum correlation (HSQC) spectrum of PaIF3NΔ20 is shown in **Figure 10**. The spectrum displays a well-folded protein based on the large chemical shift dispersion and strong backbone amide resonances with uniform intensities. The sequence of PaIF3NΔ20 was submitted to the trRosetta server for a sequence-based structure prediction. The best structure obtained for PaIF3NΔ20 shown in **Figure 11** consists of a four-stranded β-sheet and one α-helix followed the beginning of the interdomain linker. Majority of the α-helix region consists of hydrophobic and acidic residues. In addition, the predicted structure of PaIF3NΔ20 contains less unstructured regions when compared to the predicted structure of IF3N, suggesting the truncated structure is more rigid compared to the wildtype (IF3N). The structure variability suggests the first 20 amino acid residues may contribute to the overall structure of IF3N and its function. However, this predicted structure needs further refinement with chemical shift assignments and NOE data for a high-resolution structure.

A predicted full-length structure of PaIF3 is shown in **Figure 12,** which demonstrates a long highly flexible, α-helical interdomain linker. The predicted structure shows less structured regions between the α-helices and β-sheets when compared to the C-terminal domain previously isolated (PDB 6VRJ). Indicating the individual domains may change their conformation when connected through the interdomain linker. However, this predicted structure needs further refinement with chemical shift assignments and NOE data for a high-resolution structure.

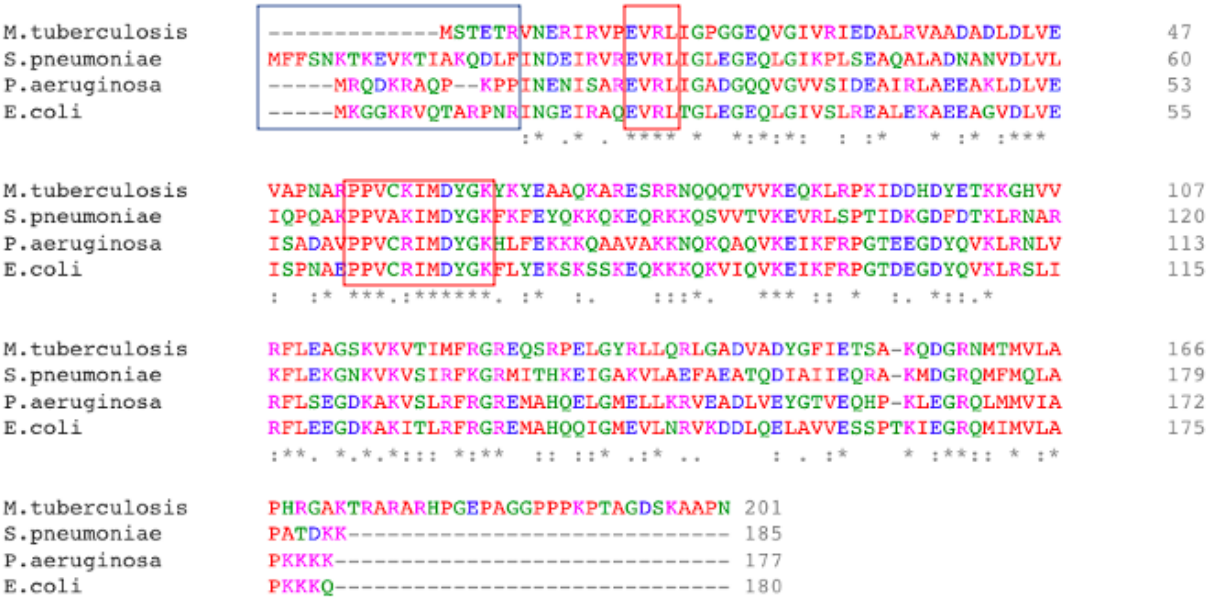

Figure 8. Sequence alignment of PaIF3 with homologs. IF3 sequences in *M. tuberculosis*, *S. pneumoniae*, and *E. coli* obtained using ClustalOmega. Highly conserved residues near the N-terminal domain are outlined in red. Amino acids with unstructured regions in the N-terminal domain highlighted in blue.

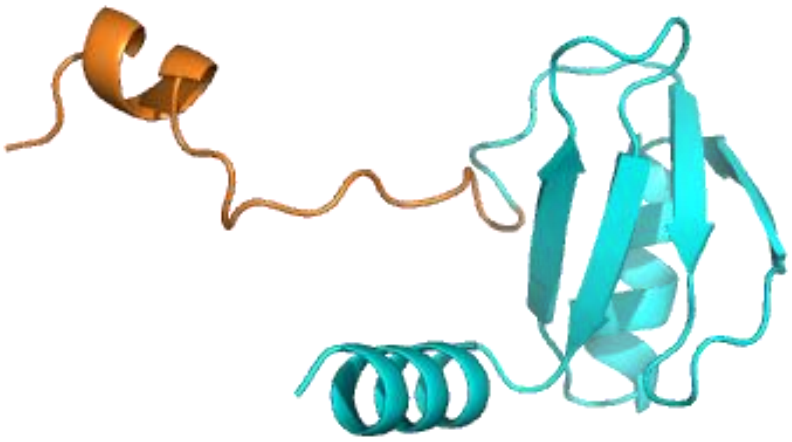

Figure 9. Three-dimensional predicted structure of the IF3N domain in *P. aeruginosa*. Estimated TM-score of 0.834. Data collected by submitting the wildtype sequence to the trRosetta server. Unstructured, truncated region highlighted in orange.

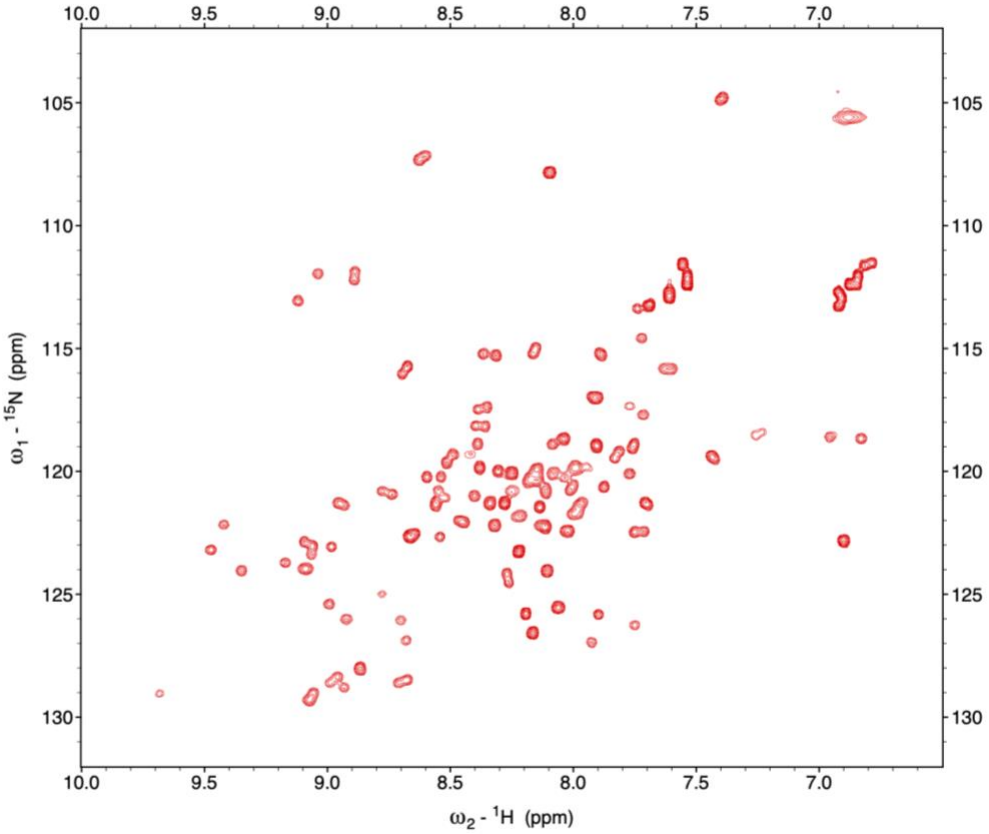

Figure 10. Two-dimensional ^{1}H-^{15}N HSQC Spectrum of PaIF3NΔ20. NMR sample prepared with 25mM potassium phosphate buffer, pH 6.5/5mM DTT/8%D_2O.

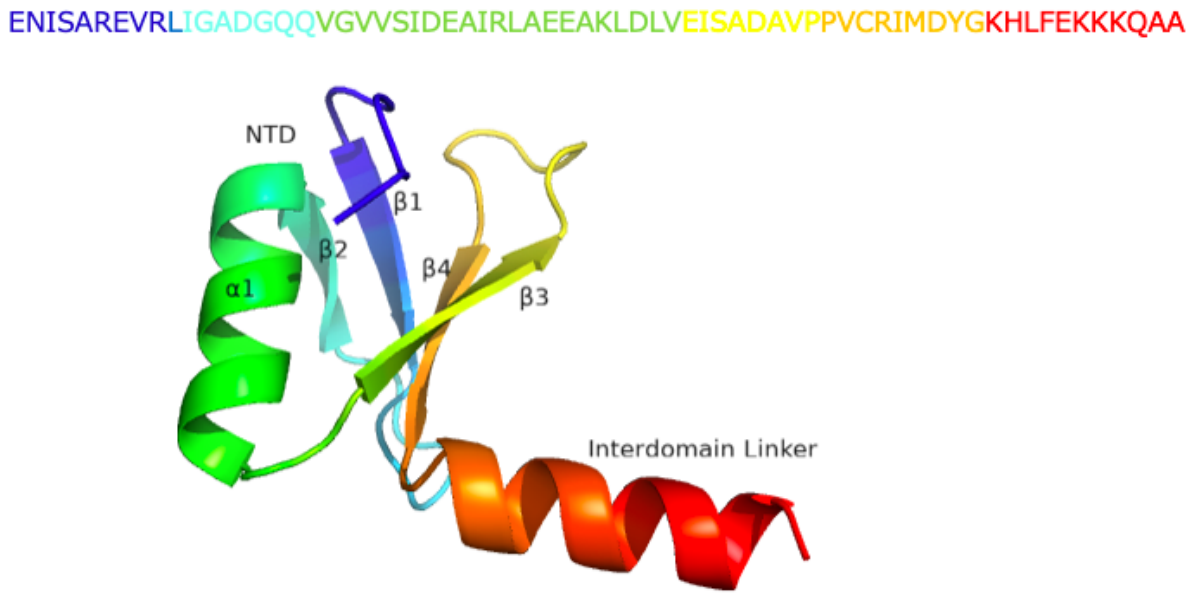

Figure 11. Three-dimensional structure predication of PaIF3NΔ20. Estimated TM-score of 0.865. Data collected by submitting the truncated sequence onto the trRosetta server. Domains labeled using PyMOL.

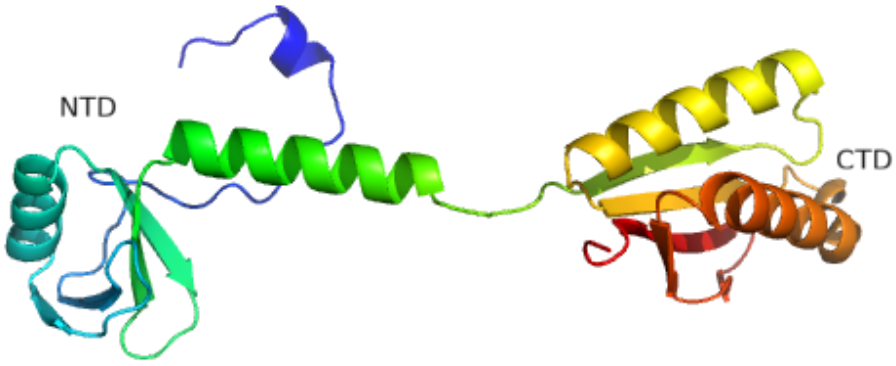

Figure 12. Three-dimensional full-length structure prediction of PaIF3. Estimated TM-score of 0.725. Data collected by submitting the amino acid sequence onto the trRosetta server. N- and C-terminal domains labeled using PyMOL.

CHAPTER IV

SUMMARY AND CONCLUSIONS

The multi-drug resistant bacterial pathogen *P. aeruginosa* is notorious for its fatal infections in immunocompromised individuals. Bacterial infections with this pathogen are particularly harder to treat because of its highly evolved resistance mechanisms to multiple antibiotics and its vast ability to develop resistance to new antibiotics during therapy, resulting in difficulty to select an appropriate antibiotic treatment and an increased risk of receiving inadequate antimicrobial therapy (Paterson and Rice, 2003). Moreover, few of the novel therapeutic strategies that have been implemented for *P. aeruginosa* have proceeded into clinical practice. This is due to a limited understanding of the host and bacteria as an integrated system and few antimicrobial targets, different from current antibiotics, have been proposed. In this research, the regulations of translation initiation factor IF1 of *P. aeruginosa* were investigated to determine a potential antimicrobial candidate. A short α-helical peptide was utilized as a functional mimic of the PaIF1 α-helix and displayed a high ability to compete with IF1 during protein synthesis by inhibiting bacterial growth in *P. aeruginosa* and other Gram-negative and Gram-positive bacteria with little to no toxicity of human cell cultures. Additionally, the PaIF1 peptide displayed an ability to reduce the effects of swarming in *P. aeruginosa*, a known virulence factor. With optimizations, these results provide an indication of novel antimicrobial peptides against the bacterial pathogen.

Although antibacterial activity of AMPs *in vitro* is potent, as presented in this research, their *in vivo* failures, stability, toxicity, and production cost have hindered their further development and clinical application. A high-throughput screening approach would provide a better understanding of the structure-function relationship of the peptide as well as aid in the further optimization of the peptide. Future studies for the PaIF1 peptide include a fluorescein-labeled protein assay to observe the cellular localization of the peptide in bacterial cells and determine its mechanism of action.

The N-domain of IF3 in *P. aeruginosa* was investigated to develop a model of a full-length structure of IF3. The two-dimensional HSQC spectrum of a truncated N-domain revealed uniform peak intensities and may indicate a well-folded protein. However, further optimization of the predicted structure via NMR is required. The structure determination of the N-domain will contribute to the structure determination of a full-length IF3, which will allow us to obtain a better understanding of the role and interactions of this protein during protein synthesis with the 30S ribosome. This in turn would contribute to the development of antimicrobial candidates against *P. aeruginosa* infections.

REFERENCES

Aldred, K.J., Kerns, R.J., Osheroff, N. Mechanism of Quinolone Action and Resistance *Biochemistry 53*(10), 1565-1574

Arenz, S., & Wilson, D. N. (2016). Bacterial Protein Synthesis as a Target for Antibiotic Inhibition. *Cold Spring Harbor perspectives in medicine*, *6*(9)

Beganovic, M., Luther, M.K., Rice, L.B., Arias, C.A., Rybak, M.J., LaPlante, K.L. (2018). A Review of Combination Antimicrobial Therapy for Enterococcus faecalis Bloodstream Infections and Infective Endocarditis. *Clinical infectious disease: an official publication of the Infectious Diseases Society of America*, *67*(2), 303–309

Braz, V.S., Furlan, J.P., Fernandes, A.F., Stehling, E.G. (2016). Mutations in NalC induce MexAB-OprM overexpression resulting in high level of aztreonam resistance in environmental isolates of Pseudomonas aeruginosa. *FEMS Microbiol*. Lett. 363

Browne, K., Chakraborty, S., Chen, R., Willcox, M.D., Black, D.S., Walsh, W.R., Kumar N. (2020). A New Era of Antibiotics: The Clinical Potential of Antimicrobial Peptides. *International Journal of Molecular Sciences*. 21(19):7047

Burrows, L. (2018). The Therapeutic Pipeline for *Pseudomonas aeruginosa* Infections. *ACS Infect. Dis.* 4(7), 1041–1047

Carter, A.P., Clemons, W.M., Brodersen, D.E., Morgan-Warren, R.J., Hartsch, T., Wimberly, B.T., Ramakrishnan, V. (2001). Crystal structure of an initiation factor bound to the 30S ribosomal subunit. Science 291:498–501

CDC. (2019). Antibiotic Resistance Threats in the United States. Atlanta, GA: U.S. Department of Health and Human Services, CDC.

Chopra, I., & Roberts, M. (2001). Tetracycline antibiotics: mode of action, applications, molecular biology, and epidemiology of bacterial resistance. *Microbiology and molecular biology reviews: MMBR*, *65*(2), 232–260

Cope, J.R., Collier, S.A., Srinivasan, K., Abliz, E., Myers, A., Millin, C.J., Miller, A., Tarver, M.E. (2015). Contact Lens–Related Corneal Infections — United States, 2005–2015. MMWR *Morb Mortal Wkly*. 65, 817–820

Das, T., Sehar, S., Manefield, M. (2013). The roles of extracellular DNA in the structural integrity of extracellular polymeric substance and bacterial biofilm development. Environ *Microbiol Rep,* 5(6):778-86

De Oliveira, D.M.P., Forde, B.M., Kidd, T.J., Harris, P.N.A., Schembri, M.A., Beatson, S.A., Paterson, D.L., Walker, M.J. (2020). Antimicrobial Resistance in ESKAPE Pathogens. *Clin Microbiol Rev.* 13;33(3)

Dreier, J., & Ruggerone, P. (2015). Interaction of antibacterial compounds with RND efflux pumps in Pseudomonas aeruginosa. *Frontiers in microbiology*, *6*, 660

Du, Z., Su, H., Wang, W., Ye, L., Wei, H., Peng, Z., Anishchenki, I., Baker, D., Yang, J. (2021). The trRosetta server for fast and accurate protein structure prediction. *Nat Protoc* **16,** 5634–5651

Fang, Z.L., Zhang, L.Y., Huang, Y.M., Qing, Y., Cao, K.Y., Tian, G.B., Huang, X. (2014). OprD mutations and inactivation in imipenem-resistant Pseudomonas aeruginosa isolates from China. Infect Genet Evol 21, 124–128

Fjell, C.D, Hiss, J.A, Hancock, R.E.W., Schneider, G. (2012). Designing antimicrobial peptides: form follows function. *Nat Rev Drug Discov* **11,** 37–51

Fourmy, D., Recht, M.I., Blanchard, S.C., Puglisi, J.D. (1996). Structure of the A site of Escherichia coli 16S ribosomal RNA complexed with an aminoglycoside antibiotic. Science. 274(5291):1367-71

Girard, G. and Bloemberg, G.V. (2008). Central role of quorum sensing in regulating the production of pathogenicity factors in *Pseudomonas aeruginosa*. *Future Micro.* 3(1)

Groß, A., Hashimoto, C., Sticht, H., Eichler, J. (2016). Synthetic Peptides as Protein Mimics. *Front Bioeng Biotechnol.*

Gualerzi, C.O., & Pon, C.L. (2015). Initiation of mRNA translation in bacteria: structural and dynamic aspects. *Cellular and molecular life sciences: CMLS*, *72*(22), 4341–4367

Guillamet, C.V., Vazquez, R., Jonas, N., Scott, M.T., Kollef, M.H. (2016). A cohort study of bacteremic pneumonia. The importance of antibiotic resistance and appropriate initial therapy? Medicine. 95(35), 4708

Hu, Y., Bernal, A., Bullard, J.M., Zhang, Y. (2016), Solution structure of protein synthesis initiation factor 1 from *Pseudomonas aeruginosa*. Protein Science, 25: 2290- 2296

Hussain, T., Llácer, J.L., Wimberly, B.T., Kieft, J.S., Ramakrishnan, V. (2016). Large-Scale Movements of IF3 and tRNA during Bacterial Translation Initiation. *Cell*, *167*(1), 133–144.e13

Jiang, K., Yan, X., Yu, J., Xiao, Z., Wu, H., Zhao, M., Yue, Y., Zhou, X., Xiao, J., Lin, F. (2020). Design, synthesis, and biological evaluation of 3-amino-2-oxazolidinone derivatives as potent quorum-sensing inhibitors of Pseudomonas aeruginosa PAO1. *Eur J Med Chem.*

Julián, P., Milon, P., Agirrezabala, X., Lasso, G., Gil, D., Rodnina, M.V, Valle, M. (2011). The Cryo-EM structure of a complete 30S translation initiation complex from *Escherichia coli. PLoS Biol*

Jurado-Martín, I., Sainz-Mejías, M., McClean, S. (2021). *Pseudomonas aeruginosa*: An Audacious Pathogen with an Adaptable Arsenal of Virulence Factors. *Int J Mol Sci.* 22(6), 3128

Kragol, G., Lovas, S., Varadi, G., Condie, B.A., Hoffmann, R., Otvos, L. (2001). The antibacterial peptide pyrrhocoricin inhibits the ATPase actions of DnaK and prevents chaperone-assisted protein folding Biochemistry, 40 (10); 3016-3026

Krause, K. M., Serio, A. W., Kane, T.R., Connolly, L.E. (2016). Aminoglycosides: An Overview. *Cold Spring Harbor perspectives in medicine*, *6*(6)

Lee, T.H., Hall, K.N., Aguilar, M.I. (2016). Antimicrobial Peptide Structure and Mechanism of Action: A Focus on the Role of Membrane Structure. *Curr Top Med Chem.* 16(1):25-39

Li, H., Luo, Y.F., Williams, B.J., Blackwell, T.S., Xie, C.M. (2012). Structure and function of OprD protein in Pseudomonas aeruginosa: from antibiotic resistance to novel therapies. *Int J Med Microbiol*. 302(2):63-8

Li, L., Palmer, S.O., Gomez, E.A., Mendiola, F., Wang, T., Bullard, J.M., Zhang, Y. (2020). ^{1}H, ^{13}C, and ^{15}N resonance assignments of translation initiation factor 3 from *Pseudomonas aeruginosa. Biomol. NMR Assign.* 14(1): 93-97

Liu Y, Shi J, Tong Z, Jia Y, Yang B, Wang Z. (2020). The revitalization of antimicrobial peptides in the resistance era. *Pharmacol Res.*

Luzzatto, L., Apirion, D., Schlessinger, D. (1968). Mechanism of action of streptomycin in E. coli: interruption of the ribosome cycle at the initiation of protein synthesis. *Proceedings of the National Academy of Sciences of the United States of America*, *60*(3), 873–880

Maar, D., Liveris, D., Sussman, J.K., Ringquist, S., Moll, I., Heredia, N., Kil, A., Bläsi, U., Schwartz, I., Simons, R.W. (2008). A single mutation in the IF3 N-terminal domain perturbs the fidelity of translation initiation at three levels. *J Mol Biol* 383:937–944

Magana, M., Pushpanathan, M., Santos, A.L., Leanse, L., Fernandez, M., Ioannidis, A., Giulianotti, M.A., Apidianakis, Y., Bradfute, S., Ferguson, A.L., Cherkasov, A., Seleem,

M.N., Pinilla, C., de la Fuente-Nunez, C., Lazaridis, T., Dai, T., Houghten, R.A., Hancock, R.E.W., Tegos, G.P. (2020). The value of antimicrobial peptides in the age of resistance. *Lancet Infect Dis.* 20(9):e216-e230.

McCoy, L.S., Xie, Y., Tor, Y. (2010). Antibiotics that target protein synthesis. Wiley Interdiscip Rev RNA. 2(2):209-32

Milón, P., & Rodnina, M.V. (2012) Kinetic control of translation initiation in bacteria, *Critical Rev. in Biochem & Mol Bio*, 47:4, 334-348

Milón, P., Maracci, C., Filonava, L., Gualerzi, C.O., Rodnina, M.V. (2012). Real-time assembly landscape of bacterial 30S translation initiation complex. *Nat Struct Mol Biol.* 19(6):609-615

Munita, J.M., Arias, C.A. (2016). Mechanisms of antibiotic resistance. *Microbiol Spectr* 4

Nakamoto, J.A., Evangelista, W., Vinogradova, D.S., Konevega, A.L., Spurio, R., Fabbretti, A., Milón, P. (2021). The dynamic cycle of bacterial translation initiation factor IF3. *Nucleic acids research*, *49*(12), 6958–6970

Wang, M., Wei, H., Zhao, Y., Shang, L., Di, L., Lyu, C., Liu, J. (2019). Analysis of multidrug-resistant bacteria in 3223 patients with hospital-acquired infections (HAI) from a tertiary general hospital in China. *Bosn J Basic Med Sci.* 19(1), 86-93

Wolter, D.J., Lister, P.D. (2013). Mechanisms of beta-lactam resistance among Pseudomonas aeruginosa. *Curr Pharm Des* 19, 209–222

Wood, T.K., Knabel, S.J., Kwan, B.W. (2013). Bacterial persister cell formation and dormancy. *Appl Environ Microbiol* 79, 7116–7121

Overhage, J., Bains, M., Brazas, M.D., Hancock, R.E. (2008). Swarming of Pseudomonas aeruginosa is a complex adaptation leading to increased production of virulence factors and antibiotic resistance. *J Bacteriol.* 190(8):2671-9

Page, M.G. (2012). The role of the outer membrane of Gram-negative bacteria in antibiotic resistance: Ajax' shield or Achilles' heel? *Handb Exp Pharmacol*. (211), 67-86

Palmer, G.C., Whitely, M. (2021). Metabolism and Pathogenicity of Pseudomonas aeruginosa Infections in the Lungs of Individuals with Cystic Fibrosis. *ASM Journals.* 3(4)

Pandey, N., & Cascella, M. (2022). Beta Lactam Antibiotics. In: StatPearls [Internet]. Treasure Island (FL): StatPearls Publishing

Pang, Z., Raudonis, R., Glick, B.R., Lin, T.J., Cheng, Z. (2019). Antibiotic resistance in Pseudomonas aeruginosa: mechanisms and alternative therapeutic strategies. Elsevier. *Biotech Adv.* 37, 177-192

Pestrak, M.J., Chaney, S.B., Eggleston, H.C., Dellos-Nolan, S., Dixit, S., Mathew-Steiner, S.S., Roy, S., Parsek, M.R., Sen, C.K., Wozniak, D.J. (2018). *Pseudomonas aeruginosa* rugose small-colony variants evade host clearance, are hyper-inflammatory, and persist in multiple host environments. *PLoS Pathog*. 14

Paterson, D.L., & Rice, L.B. (2003). Empirical antibiotic choice for the seriously ill patient: are minimization of selection of resistant organisms and maximization of individual outcome mutually exclusive? *Clin Infect Dis* 36:1006–1012

Pushpanathan, M., Gunasekaran, P., Rajendhran, J. (2013). Antimicrobial peptides: versatile biological properties. *Int J Pept.*

Reece, E., Segurado, R., Jackson, A., McClean, S., Renwick, J., Greally, P. (2017). Co-colonisation with *Aspergillus fumigatus* and *Pseudomonas aeruginosa* is associated with poorer health in cystic fibrosis patients: an Irish registry analysis. *BMC Pulm Med.* 17, 70

Rodnina M. V. (2018). Translation in Prokaryotes. *Cold Spring Harbor perspectives in biology*, *10*(9)

Rossi, E., La Rosa, R., Bartell, J.A., Marvig, R.L., Haagensen, J.A.J., Sommer, L.M., Molin, S., Johansen, H.K. (2021). *Pseudomonas aeruginosa* adaptation and evolution in patients with cystic fibrosis. *Nat Rev Microbiol* 19, 331–342

Sardar, A.H., Das, S., Agnihorti, S., Kumar, M., Ghosh, A.K., Abhishek, K., Kumar, A., Purkait, B., Ansari, M.Y., Das, P. (2013). Spinigerin induces apoptotic like cell death in a caspase independent manner in Leishmania donovani, *Exp Parasitology*,135(4); 715-725

Scharff, L.B., Childs, L., Walther, D., Bock, R. (2011). Local absence of secondary structure permits translation of mRNAs that lack ribosome-binding sites. *PLoS Genet.*

Schrödinger, L., & DeLano, W. (2020). *PyMOL*. Retrieved from http://www.pymol.org/pymol

Sette, M., van Tilborg, P., Spurio, R., Kaptein, R., Paci, M., Gualerzi, C.O., Boelens, R. (1997). The structure of the translational initiation factor IF1 from *E.coli* contains an oligomer-binding motif. *The EMBO Journal*, 16, 1436-1443

Sievers, F., Wilm, A., Dineen, D., Gibson, T.J., Karplus, K., Li, W., Lopez, R., McWilliam, H., Remmert, M., Söding, J., Thompson, J.D., Higgins, D.G. (2011). Fast, scalable generation of high-quality protein multiple sequence alignments using Clustal Omega. *Mol. Syst. Biol.* 7:539

Simonetti A, Marzi S, Myasnikov AG, Fabbretti A, Yusupov M, Gualerzi CO, Klaholz BP. (2008). Structure of the 30S translation initiation complex. *Nature* 455, 416–420

Soto, S.M. (2013). Role of efflux pumps in the antibiotic resistance of bacteria embedded in a biofilm. *Virulence* 4:3, 223-229

Suetens, C., Latour, K., Kärki, T., Ricchizzi, E., Kinross, P., Moro, M.L., Jans, B., Hopkins, S., Hansen, S., Lyytikäinen, O., Reilly, J., Deptula, A., Zingg, W., Plachouras, D., Monnet, D.L. (2018). The Healthcare-Associated Infections Prevalence Study Group. Prevalence of healthcare-associated infections, estimated incidence and composite antimicrobial resistance index in acute care hospitals and long-term care facilities: results from two European point prevalence surveys, 2016 to 2017. *Euro Surveill.* 23(46)

Valdez, N., Hughes, C., Palmer, S.O., Sepulveda, A., Dean, F.B., Escamilla, Y., Bullard, J.M., Zhang, Y. (2021). Rational Design of an Antimicrobial Peptide Based on Structural Insight into the Interaction of Pseudomonas aeruginosa Initiation Factor 1 with Its Cognate 30S Ribosomal Subunit. *ACS Infectious Diseases*, *7*(12), 3161-3167

Van den Bergh, B., Fauvart, M., Michiels, J. (2017). Formation, physiology, ecology, evolution, and clinical importance of bacterial persisters. FEMS Microbiol Rev 41, 219–251

BIOGRAPHICAL SKETCH

Nicolette Valdez was born in Laredo, Texas. She earned her Bachelors degree in 2019 at Texas A&M International University (TAMIU) where she majored in biology with a minor in chemistry. She was accepted into the University Honors Program at TAMIU where she was able to complete an undergraduate research thesis and studied the phylogenetic distribution of Arsenic and Antimony tolerant bacteria of the Chacon Creek Flood Plain working with Dr. Monica Mendez. In 2022, she obtained a Master's Degree in Biochemistry and Moleculary Biology at the University of Texas Rio Grande Valley where she studied the structures and regulations of translation initiation factors in protein biosynthesis to develop antimicrobial targets working with Dr. Yonghong Zhang. She received a presidential graduate research assistantship with UTRGV to be used toward her tuition. During her graduate studies she was also a teaching assistant for the General Biology I and Microbiology laboratories where she mentored undergraduate students in the understanding of techniques related to the field of study. For contact information please email nicolette.15valdez@gmail.com.